

Solution Structural Study of BlaI: Implications for the Repression of Genes Involved in β -Lactam Antibiotic Resistance

Hélène Van Melckebeke^{1†}, Christelle Vreuls^{2,3†}, Pierre Gans¹
Patrice Filée², Gabriel Llabres³, Bernard Joris² and
Jean-Pierre Simorre^{1*}

¹Institut de Biologie
Structurale-Jean-Pierre Ebel
CEA-CNRS-UJF, 41 Avenue
Jules Horowitz, 38027 Grenoble
Cedex 1, France

²Centre d'ingénierie des
protéines, Institut de Chimie
B6A, Université de Liège
Sart-Tilman B4000, Belgium

³Laboratoire de Physique
Expérimentale, Département de
Physique, Bat B5, Université de
Liège, Sart Tilman B4000
Belgium

β -Lactamase and penicillin-binding protein PBP2' mediate staphylococcal resistance to β -lactam antibiotics, which are otherwise highly clinically effective. Two repressors (BlaI and Mecl) regulate expression of these inducible proteins. Here, we present the first solution structure of the 82 amino acid residue DNA-binding domain of *Bacillus licheniformis* BlaI which is very similar in primary sequence to the medically significant Staphylococcal BlaI and Mecl proteins. This structure is composed of a compact core of three α -helices and a three-stranded β -sheet typical of the winged helix protein (WHP) family. The protein/DNA complex was studied by NMR chemical shift comparison between the free and complexed forms of BlaI. Residues involved in DNA interaction were identified and a WHP canonical model of interaction with the operators is proposed. In this model, specific contacts occur between the base-pairs of the TACA motif and conserved amino acid residues of the repressor helix H3. These results help toward understanding the repression and induction mechanism of the genes coding for β -lactamase and PBP2'.

© 2003 Elsevier Ltd. All rights reserved.

Keywords: β -lactamase repressor BlaI; NMR spectroscopy; winged helix protein; protein–DNA interaction; antibiotic resistance

*Corresponding author

Introduction

To date, the nosocomial spread of the bacterial strains resistant to antibiotics has become a major public health concern.^{1,2} Many strains have become resistant to β -lactam antibiotics, by either (i) the expression of a specific hydrolase, the β -lactamase, which inactivates β -lactam antibiotics by hydrolyzing their endocyclic amide bond, or (ii) the production of an alternative transpeptidase penicillin-binding protein (PBP2'), insensitive to penicillin inhibition.³ Although β -lactamase and PBP2' have different structures and functions, their synthesis is regulated by a similar repression mechanism.

The expression of the β -lactamase, BlaZ in *Staphylococcus aureus* or BlaP in *Bacillus licheniformis* 749/I, is under the control of three genes: *blaI*, *blaR1* and *blaR2*. The first two genes are clustered in an operon and form a divergon with the *blaZ/blaP* gene (Figure 1A). The *blaR2* gene is not linked to the divergon, and it has not been identified yet.⁴ The BlaR1 membrane-bound protein is a penicillin receptor, which detects the presence of the β -lactam antibiotic outside the cell.⁵ BlaI is a cytoplasmic protein, which specifically recognizes DNA operator sequences in the intergenic region between the *blaP/blaZ* and *blaI-blaR1* genes (Figure 1A). In absence of a β -lactam antibiotic, BlaI is bound to its operator sequence as a dimer and acts as a repressor for the *blaP/blaZ* gene expression. The presence of β -lactam antibiotics leads to the acylation of BlaR1⁵ and in turn to the transmission of an intracellular signal whose final target is BlaI itself. Consequently, BlaI is released from its operator and this leads to a high level of β -lactamase production. The *S. aureus* and

Supplementary data associated with this article can be found at doi: 10.1016/j.jmb.2003.09.005

† H.V.M. and C.V. contributed equally to this work.

Abbreviations used: WHP, winged helix protein.

E-mail address of the corresponding author:
jean-pierre.simorre@ibs.fr

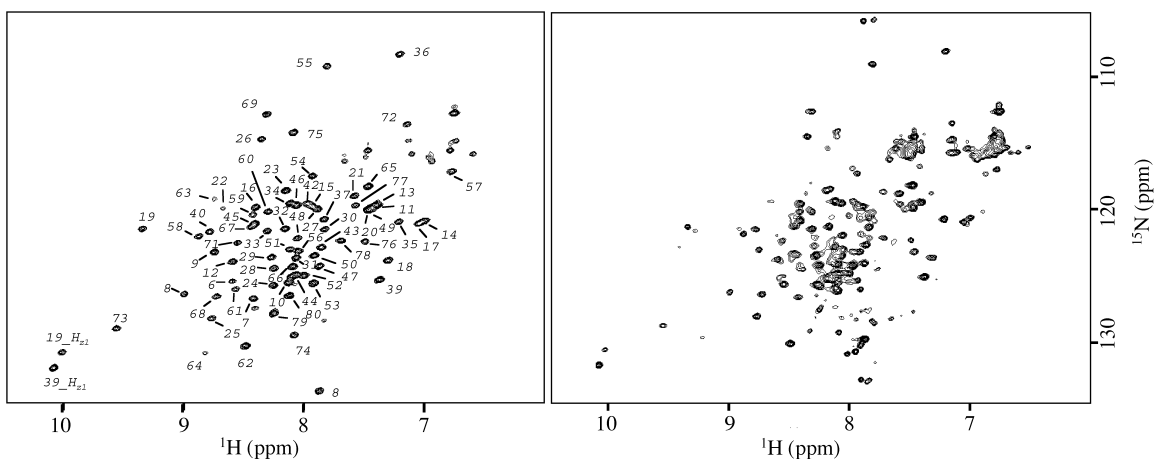


Figure 2. Comparison of the ^{15}N HSQC spectra at 25 °C of BlaI N-terminal domain (BlaI-NTD) and of full-length BlaI. Left: BlaI-NTD spectrum with assignment obtained for residues 6–81. Right: spectrum of the complete protein BlaI. Except for residue 81, all BlaI-NTD resonances are observed in the same positions, indicating that the N-terminal part of the protein forms an independent and structured domain. The resonances corresponding to the C-terminal domain (83–128) are poorly resolved and are mainly located in a region characteristic of extended structure.

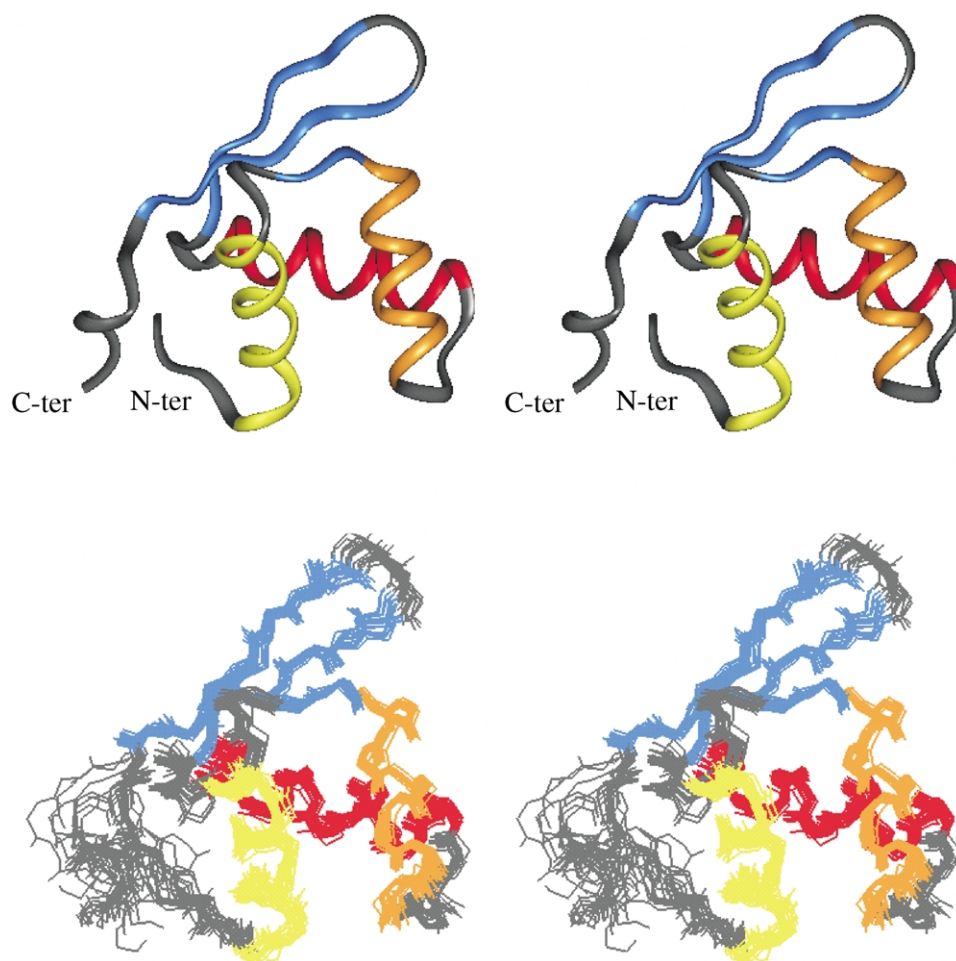


Figure 3. NMR structures of BlaI-NTD (1–82). Secondary structures are colored: H1 in yellow, H2 in orange, H3 in red and the three strands of the β -sheet in blue. Top: stereo view of the ribbon backbone diagram of the lowest-energy structure. Bottom: stereo view of the backbone diagram of the 19 refined low-energy structures. Backbone heavy atoms were used for superimposition.

that the N-terminal part constitutes an independent structural domain. Only a few resonances of *BlaI*-NTD differ between the two spectra, and those correspond to the residue neighboring the cleavage site (Lys81). The resonances corresponding to the C-terminal domain (82–128) are broad and poorly resolved, suggesting that this domain could be less structured or more mobile than the N-terminal domain.

The *BlaI*-NTD structure was solved using two- and multidimensional NMR spectroscopy, making use of uniformly ^{15}N , $^{13}\text{C}/^{15}\text{N}$ and $^2\text{H}/^{13}\text{C}/^{15}\text{N}$ -labeled proteins. Nearly complete ^1H , ^{13}C and ^{15}N assignments were obtained using standard resonance assignment procedures. The few missing assignments correspond to the N and C-terminal ends (residues 1–4, and 82).

For structure calculation, a total of 1252 interproton, 110 dihedral and 97 chiral restraints were used. The distance constraints contain 596 intra-residue, 205 sequential, 87 medium-range, 145 long-range and 219 ambiguous correlations derived from 2D, 3D, and 4D nuclear Overhauser effect spectroscopy (NOESY) spectra. The dihedral ψ and ϕ angle restraints were deduced from TALOS, using backbone chemical shift values. At the final stage, 80 conformers were calculated, and the conformers with the lowest-energy functions were selected to be refined. A ribbon diagram of the lowest-energy structure and a superposition of the final ensemble of 19 simulated annealing structures are shown (Figure 3).

Ensemble analysis of *BlaI*-NTD backbone stereochemical quality was done with NMR-PROCHECK.¹² Over 99% of the dihedral angles were found in the most favored and additional allowed regions of the Ramachandran plot. Structural conformations of residues 1–4 and 79–82 are poorly defined, due to the lack of assignment for residues 1–4 and 82, or to the small number of NOE constraints for residues 79–81. Heteronuclear NOEs (Supplementary Material) confirm that the N and C-terminal parts of the protein are rather mobile. For statistics, we consider only the rigid core of *BlaI*-NTD (residues 5–78). For these residues, we obtained an average of 16.4 restraints per residue. A good agreement with the experimental restraints is reflected by the low experimental energy level. There is no distance restraints violation greater than 0.1 Å. The backbone and heavy-atom root-mean-square deviation (rmsd) values calculated for *BlaI*-NTD 5–78 with respect to the mean coordinates are 0.63 (± 0.17), and 1.07 (± 0.18) Å, respectively. A summary of the restraint and structural statistics is presented in Table 1.

The *BlaI*-NTD 3D structure consists of a three-stranded β -sheet (S1, Ser23-Asn25; S2, Leu57-Glu62; and S3, Val65-Pro70) packed against three α -helices (H1, Asp9-Lys20; H2, Thr26-Thr36; and H3, Pro41-Lys53) arranged in the order H1-S1-H2-T1-H3-S2-W1-S3. S2 and S3 form an antiparallel hairpin (loop called wing W1: Gly63-Arg64) and

S1 is connected antiparallel to S3. T1 (Ser37-Ser40) is a type I turn connecting H2 and H3. The α -helices and the β -sheet form a well-defined and compact core. This tertiary arrangement belongs to the winged helix proteins (WHP) family, which is a member of the DNA recognition helix-turn-helix superfamily.^{13,14} Among the WHP, the relative orientation of the secondary structures is variable due to the differences in the length of the T1 turn connecting H2 and H3, and in the length of the wing W1. Comparison of the structure of *BlaI*-NTD with other WHP proteins was made using the DALI search algorithms.¹⁵ The most similar 3D structures are those of E2F4, SMTB, ADAR1, LexA, MarR, FokI, DTXR, and Genesis, all of them being DNA recognition domains. It is interesting to note that the MarR protein is also involved in a mechanism of antibiotic resistance.¹⁶ Although no sequence homology could be detected by primary sequence similarity searches, all these proteins present a central core similar to that of *BlaI*-NTD. Whereas their helices can be of significantly different lengths, angles between the three α -helices are conserved. The main differences observed for these proteins are localized in the wing region. Some of the WHP proteins like Genesis have a long and flexible W1 wing, as revealed by heteronuclear NOE measurements.¹⁷ In the case of *BlaI*-NTD, wing W1 is short (residues 63–64). Heteronuclear NOE data (Supplementary Material) show no particular mobility for residues neighboring W1.

A high degree of sequence homology exists between *B. licheniformis* *BlaI* and *S. aureus* *Mecl*, especially for the non-polar core residues. In particular, many of the buried residues forming the core of the structure are identical or similar (*BlaI*/*Mecl*) between *BlaI* and *Mecl*: (H1) Ala10, Val14,

Table 1. Structural statistics

NMR-derived restraints	1362
Interproton restraints	1252
Intraresidue restraints	596
Interresidue restraints	437
Sequential restraints	205
Medium-range restraints	87
Long-range restraints	145
Hydrogen bond restraints	0
Ambiguous restraints	219
Dihedral angle restraints	110
Chiral restraints	97
Average rms deviations from the mean coordinates (Å) ^{a,b}	
Backbone heavy-atoms:	0.63 \pm 0.17
All heavy-atoms:	1.07 \pm 0.18
Ramachandran analysis (%) ^{b,c}	
Residues in most favoured regions:	85.6
Residues in additional allowed regions:	13.7
Residues in generously allowed regions:	0.2
Residues in disallowed regions:	0.5

^a Statistics were made for residues 5–78 (see the text).

^b Average for the 19 lowest-energy structures.

^c Only non-Gly and non-Pro residues were assessed with PROCHECK-NMR.

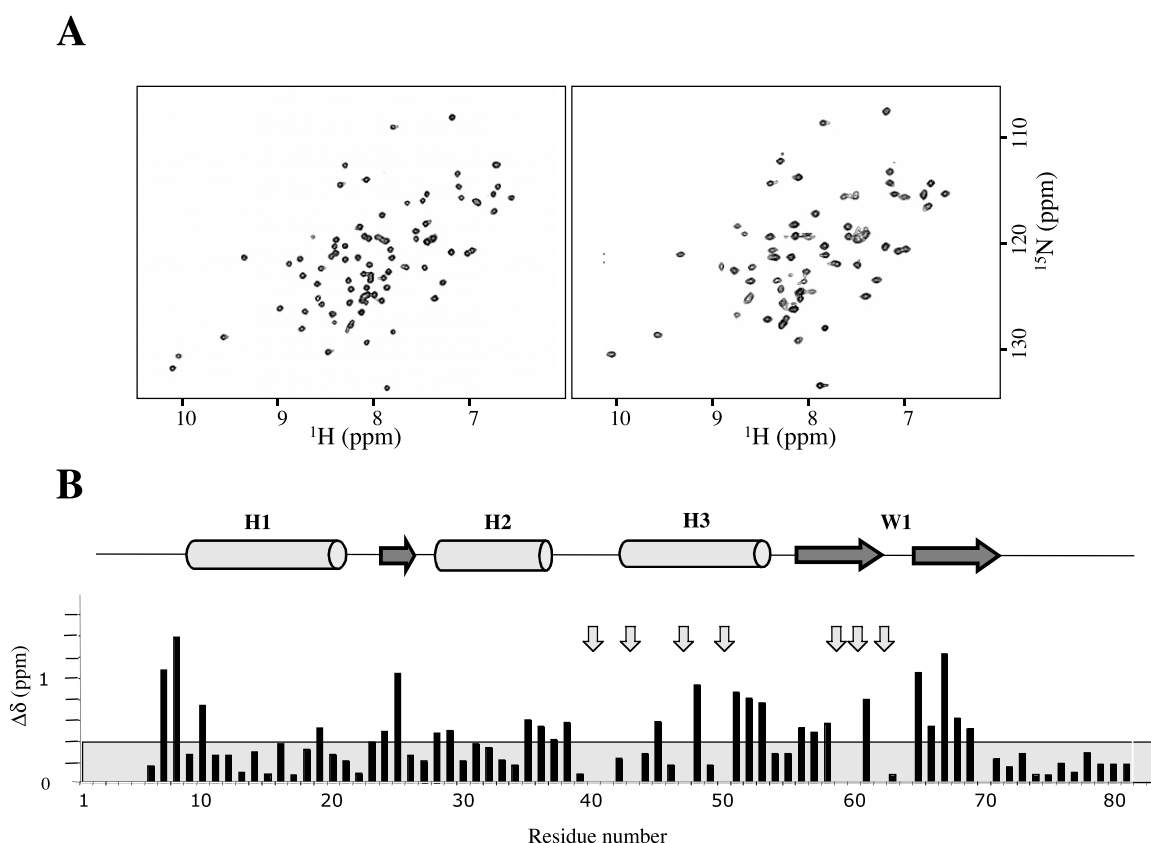


Figure 4. Chemical shift mapping of BlaI-NTD in interaction with DNA. A, ^{15}N HSQC spectra recorded at 25 °C. Left: BlaI-NTD spectrum in absence of DNA. Right: BlaI-NTD/DNA complex spectrum. The 24-mer palindromic DNA was added to the sample to reach a protein/DNA_{duplex} ratio of 1/2. (B) Graph of the chemical shift variations between the DNA free BlaI-NTD and the BlaI-NTD/DNA complex *versus* residue number. The vertical axis corresponds to $(|\delta^1\text{H}| \times |\gamma_{\text{H}}/\gamma_{\text{N}}| + |\delta^{15}\text{N}|)$ measured on the spectra presented in A. Arrows represent amino proton resonances that have been broadened and not assigned in the complexed form. The absence of a bar indicates the presence of a proline residue or an unmeasured shift due to overlap. The limit between weak and strong chemical shift variations has been fixed to 0.4 ppm.

Met15, Ile18, Trp19, (H2) Val/Ile29, Ile/Val30, Glu32, Leu/Ile33, (H3) Ile44, Leu/Ile48, Leu51, (β -sheet) Leu/Ile57, Tyr68, Ile72. Since there is no deletion or insertion necessary to align BlaI and MecI, the secondary structures predicted for MecI have the same length as for BlaI. All these data support the conclusion that MecI also belongs to the WHP family, and that its fold is very close to the BlaI structure.

DNA recognition by the repressors BlaI and MecI

For some of the WHP proteins with a BlaI-NTD similar fold listed above, the protein–DNA complex has been investigated by X-ray crystallography, NMR or computational tools.¹³ For all of them, the same DNA interaction mode has been reported. Helix H3, called the recognition helix, is presented to the major groove of the DNA, and makes specific contacts with the base-pairs. The wings (in particular W1) and the protein N-terminal part also make contacts with the minor groove of the DNA. Unlike this WHP canonical mode of

DNA recognition, the WHP RFX1 makes most of the contacts with the DNA major groove *via* wing W1.¹⁸ The so-called recognition helix H3 overlies the minor groove, and there is no contact between the N-terminal part of the protein and the DNA.

To investigate the BlaI–DNA recognition mode, the BlaI–DNA interaction surface was determined using the NMR chemical shift perturbation method. The method detects protein residues that are interacting directly, or that undergo conformational changes upon binding. ^{15}N -HSQC spectra of *B. licheniformis* BlaI-NTD were recorded with increasing amounts of DNA for both the 30-mer DNA corresponding to the *B. licheniformis* BlaI operator op1, and a palindromic 24-mer DNA based on the symmetric consensus sequence of the *mec* and *bla* operators. Results obtained with the palindromic 24-mer DNA are shown in Figure 4 and are similar to the results obtained with the 30-mer DNA (data not shown).

Since the ^{15}N -HSQC spectra of DNA-free BlaI-NTD, and of DNA-bound BlaI-NTD share many similarities (Figure 4A), the amide ^1H and ^{15}N chemical shifts of the N-terminal domain of DNA-bound

BlaI-NTD were assigned by reference to the free protein assignments. This comparison shows that BlaI-NTD does not undergo major structural rearrangements upon binding to DNA. The ^{15}N , ^1H chemical shift and intensity changes for backbone amide groups are given (Figure 4B). Significant chemical shift or intensity changes can be observed in the protein N-terminal part (Ile7 and Ser8), all along helix H3 (Ser40, Thr43, Met47, Leu48, Arg50, Leu51, and Ile52), and in the β -sheet, especially next to wing W1 (Asn25, His59, His60, Lys61, Glu62, Val65, and Val67). All the residues affected upon binding can be highlighted on the BlaI-NTD structure. They define a DNA-binding surface located on a single side of BlaI-NTD. This surface can be superimposed nicely with the positively charged region of the protein electrostatic surface (Figure 5A). The residues of the BlaI-NTD N-terminal part that are affected upon binding demonstrate the functional importance of the repressor N-terminal part in DNA-binding. This result is consistent with former DNA footprinting studies showing that a BlaI repressor mutant carrying a six amino acid deletion (Lys3-Ser8) within its N-terminal region had lost its ability to bind the operator.⁷ Mutation of lysine 4 to alanine also severely reduces the BlaI DNA-binding ability.¹⁹ The crucial role of the N-terminal domain and the shape of the electrostatic and interaction surfaces are not consistent with RFX1-DNA recognition mode, where there is no interaction between the N-terminal part of the protein and the DNA. On the contrary, they are in good agreement with a canonical WHP-DNA interaction, as described for E2F4.²⁰ Furthermore, the distances separating helix H3, wing W1, and the N-terminal ends that interact with DNA are quite equal for BlaI and E2F4. We therefore propose a model for the interaction between the repressors BlaI and MecI and their operators by comparison with the structure of the E2F4-DNA complex (Figure 5B). In this model, helix H3 interacts with the major groove of the operator. Other DNA-protein contacts occur *via* wing W1 and in the N-terminal part. Precise position of the contacts between the amino acid residues of BlaI and MecI and the base-pairs must still be investigated *via* a high-resolution structure of the DNA-repressor complexes.

Biological implication: insights about the BlaI and MecI repression mechanism

It has been reported that BlaI and MecI could corepress β -lactamase and PBP2' gene expression in *S. aureus*.⁹ In the same way, *B. licheniformis* BlaI interacts with *S. aureus* *mec* operator, as highlighted by gel mobility-shift assay (C. V., unpublished results). To explain this *mec/bla* corepression, the sequence homology for both the repressors and the DNA operator sequences of *S. aureus* and *B. licheniformis* was investigated. The primary structure alignment between *B. licheniformis* BlaI and *S. aureus* MecI and BlaI (Figure 5D) shows

that all H3 residues pointing outside the protein, and therefore probably implicated in DNA recognition (Lys42, Thr46, Arg50 and Lys53), are totally conserved among the BlaI and MecI repressors. These residues are either positively charged or able to form specific hydrogen bonds with the base-pairs. The existence of a totally conserved DNA palindromic motif (TACA) in the *mec* and *bla* operators in *S. aureus* and *B. licheniformis* has been highlighted previously (Figure 1).⁷ In our interaction model, the conserved residues in BlaI and MecI helix H3 make specific contacts with this TACA motif (Figure 5C). Interestingly, this model locates well-conserved positive residues (His59, His60, and Lys61, next to W1) facing an also conserved AT base-pair. Furthermore, locating two BlaI-NTD monomers on the two symmetric TACA motifs along the operator places the C-terminal parts of the two monomers pointing in a convenient orientation for dimerization contacts. Thus, we propose a repression mechanism, in which the repressor helix H3 makes specific contacts with the TACA motif of the operator sequence. This model is able to explain the corepression of the *mec* and *bla* genes.

Although the *S. aureus* and *B. licheniformis* BlaI share the same DNA-binding features, they exhibit different induction mechanisms. In *S. aureus*, the presence of the β -lactam inducer outside the cell results in the proteolytic cleavage of the repressor between residues N101 and F102,²¹ leading to the loss of its ability to dimerize. As pointed out above, the BlaI-NTD 3D-structure is not or slightly modified when compared to that of the wild-type BlaI, whereas the decrease of affinity between BlaI and BlaI-NTD in *B. licheniformis* is about 500–1000 times.⁷ The SmtB Zn(II) sensing metallo-regulated repressor is a WHP whose DNA-binding affinity is in the same range as BlaI-DNA affinity. The binding of a zinc ion to its C-terminal domain promotes the disassembly of the SmtB-DNA complex through a loss of affinity of about 1000.^{22,23} The binding of a co-activator to the C-terminal domain, as in SmtB, is not the only way to inhibit the repressor activity of a winged-helix transcriptional regulator. For example, in the case of *Escherichia coli* MarR, the binding of two salicylate groups close to the DNA-binding α -helix inhibits the MarR activity.¹⁶ To investigate the role of the C-terminal domain in BlaI-DNA interaction, a chemical shift mapping experiment was carried out for the dimeric full-length BlaI in the same conditions as for the monomeric BlaI-NTD (Supplementary Material). Two interesting observations can be derived from this study. First, a similar chemical shift perturbation pattern is obtained for the residues of the N-terminal domain. Second, no significant modifications of the resonances of the C-terminal domain are observed. This suggests that the interaction mode between BlaI-NTD and the DNA is not influenced by the presence of the C-terminal domain. The BlaI/MecI dimerization C-terminal domain is,

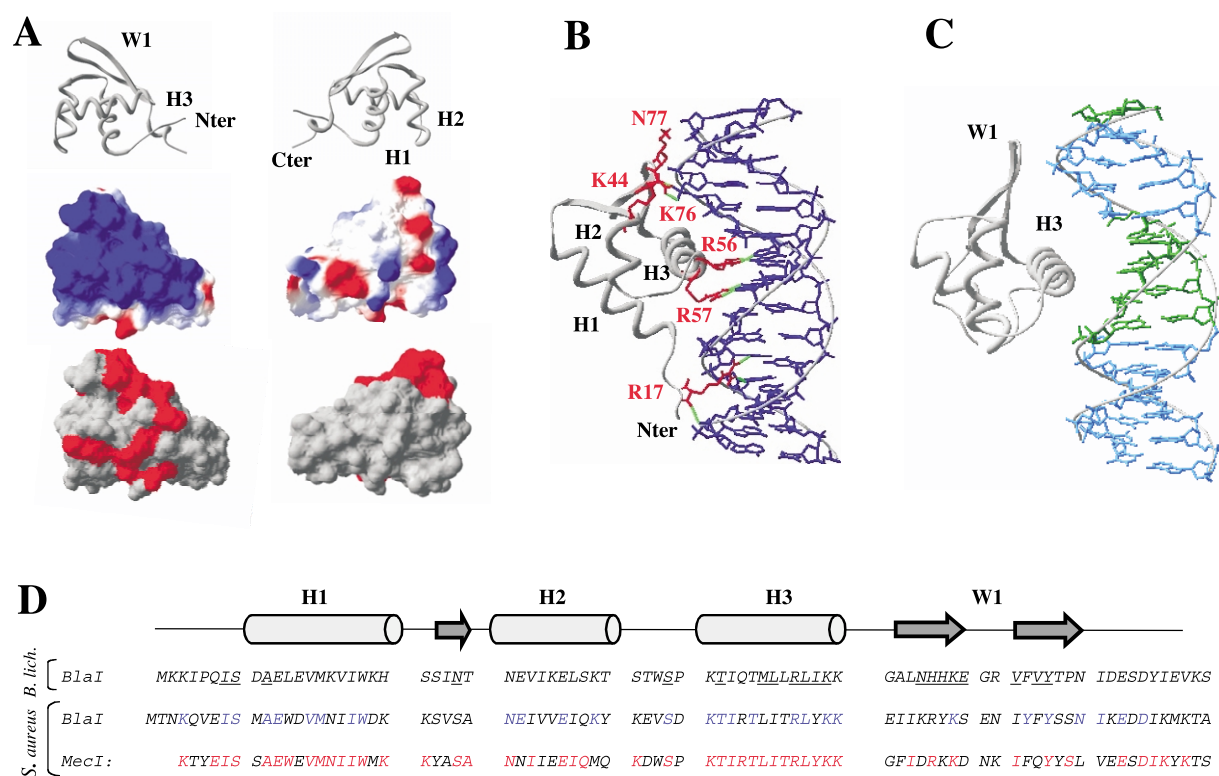


Figure 5. Comparison of the region involved in the protein/DNA complex for E2F4 and BlaI-NTD. A, Electrostatic surface of BlaI and surface mapping of the region affected by the DNA interaction. On top, ribbon representation of BlaI-NTD structure in a front and back orientation. In the middle, surface electrostatic potential is colored in red (positive) and blue (negative). The calculations were performed using the Swiss-PDB viewer (version 3.7). At the bottom, chemical shift variations ($|\delta^1\text{H}| \times |\gamma_{\text{H}}/\gamma_{\text{N}}| + |\delta^{15}\text{N}|$) superior to 0.4 ppm (see Figure 4B) are indicated in red on the BlaI-NTD surface. B, Structure of E2F4/DNA complex.²⁰ Side-chains involved in a hydrogen bond with the DNA are indicated in red and the H-bonds in green. Helix H3 forms direct H-bonds with the bases of the DNA (Arg56 and Arg57) as well as the N terminus part (Arg17). The winged helix and the turn between H1 and H2 form H-bonds with the phosphate and the sugar of the DNA (Lys44 and Asn77). Note that the residue numbering of E2F4 is quite different from that of BlaI where the H3 helix extends between the residues 41 and 53. C, Interaction model of the complex BlaI-NTD/DNA derived from the E2F4/DNA complex. BlaI-NTD structure was superimposed with E2F4 structure. Totally conserved nucleotides presented in the consensus sequence of Figure 1 are colored in green. D, Sequence alignment of *B. licheniformis* BlaI, and *S. aureus* BlaI and MecI. Residues indicated in blue correspond to amino acid residues conserved between BlaI of *B. licheniformis* and *S. aureus*. Residues indicated in red are conserved between BlaI and MecI of *S. aureus*. The highlighted residues correspond to the residues affected by the DNA interaction (determined by the *B. licheniformis* BlaI chemical shift mapping).

however, essential to obtain a DNA-binding protein of high affinity, probably placing the two DNA-binding domains in a favorable conformation for DNA contacts.

Conclusion

The 3D solution structure of *B. licheniformis* BlaI DNA-binding domain presented in this study reveals that BlaI is a member of the WHP family. *S. aureus* BlaI and MecI share also a similar WHP fold. Chemical shift mapping experiments highlighted that BlaI presents the canonical DNA recognition mode. The C-terminal part of the protein is involved in dimerisation, but not in DNA interaction. The N-terminal part is a winged helix motif, interacting *via* its N-terminal part, helix H3 and wing W1. A model of the BlaI/MecI DNA

interaction is proposed. In this model, specific contacts occur between the base-pairs of the TACA motif and conserved amino acid residues of the repressors helix H3. These results help understanding the mechanism by which the BlaI/MecI repressor regulates *blaP/blaZ/mecA* expression.

Materials and Methods

Plasmids and DNA manipulations

PET22b (Novagen) was used as vector for the over-expression of the BlaI and BlaIGM2 products. The construction of plasmids pET22bblaIWT and pET22b-blaIGM2 has been described.⁴ The GM2 mutation (M⁹⁷V⁹⁸/IL) is located in the C-terminal domain of BlaI. For BlaI-NTD production, the GM2 mutant was preferred due to its better over-expression yield.

Protein overexpression and purification

The uniformly ^{15}N -labeled BlaI sample was prepared by growing *E. coli* BL21(DE3) pLys containing the corresponding recombinant pET22b plasmid in an optimal M9 minimal medium without Casamino acids. In this medium, the only source of nitrogen was [^{15}N]ammonium chloride and the culture medium contained 18 mM $^{15}\text{NH}_4\text{Cl}$, 35 mM unlabeled glucose, 100 $\mu\text{g}/\text{ml}$ of ampicillin, 30 $\mu\text{g}/\text{ml}$ of chloramphenicol, 5 μM biotin, 7 μM thiamin, 13 μM FeSO_4 , 0.5 mM MgSO_4 , 0.01% (w/v) cholin chloride, 0.001% (w/v) folic acid, 0.002% (v/v) pyridoxal, 0.0001% (w/v) riboflavin and 0.01% (w/v) niacinamid. Cells were grown at 37 °C to an $A_{600\text{ nm}}$ of 0.7 and isopropyl β -D-galactosidase (IPTG) was then added to a final concentration of 1 mM. Overnight-induced cells were then harvested by centrifugation, lysed and purified.⁴ The final yield of purified ^{15}N -labeled protein was 6 mg per liter of cell culture and the isotopic labeling was 94% as determined by mass spectrometry.

The uniformly $^{15}\text{N}/^{13}\text{C}$ -labeled BlaIGM2 sample was produced according to the same procedure, apart from the fact that M9 minimal medium was replaced by the Silantes OD2-CN medium (Silantes GmbH, Gollierstrasse 70C, D-80339 Munchen). The final yield of purified labeled protein was 20 mg/l of cell culture and the percentage of isotopic labeling was 99%.

Uniformly $^{15}\text{N}/^{13}\text{C}/^2\text{H}$ -labeled BlaIGM2 sample was produced using the optimized M9 medium in which water had been replaced by $^2\text{H}_2\text{O}$ and with $^{15}\text{NH}_4\text{Cl}$ and ^{13}C glucose concentrations of 18 mM and 10 mM, respectively. The final yield of purified labeled protein was 4 mg per liter of cell culture and the percentage of deuterium labeling was approximately 75%.

Papain digestion and BlaI-NTD purification

Purified BlaI or BlaIGM2 were dialysed against a buffer containing 50 mM Hepes (pH7), 100 mM NaCl, 1 mM EDTA and was digested overnight using 1% mol/mol papain at 28 °C. After this time, the cleavage was complete and the protein digest was applied to an S-Sepharose-Fast-Flow column equilibrated in buffer A (50 mM Hepes (pH7), 100 mM NaCl, 1 mM EDTA, 5% (v/v) glycerol). BlaI-NTD was eluted with 1 M NaCl in the same buffer. The BlaI-NTD containing fractions were pooled, dialyzed exhaustively against 50 mM sodium phosphate (pH7.6), 200 mM KCl, 1 mM NaN_3 , 0.1 mM Pefabloc and then concentrated to a final protein concentration of 0.5 mM by ultrafiltration with a Centricon (cut-off 5 kDa, Amicon, Brussels, Belgium).

Amino N-terminal sequencing of BlaI-NTD was carried out using a Procise 492 pulsed liquid phase protein sequencer (Applied Biosystems) with 20–30 pmol of protein.

Band-shift assays

Gel retardation experiments were realized as described.²⁴

NMR sample preparation

NMR samples of BlaI-NTD were prepared at a concentration of 0.75 mM in 75 mM sodium phosphate buffer (90% H_2O , 10% $^2\text{H}_2\text{O}$), 300 mM KCl, pH 7.6. For the full-length protein, an extensive microdrop study was car-

ried out to optimize the buffer conditions and prevent aggregation observed at high concentration.²⁵ Aggregation was avoided by adding 300 mM glycine and 240 mM NaCl to the buffer used for BlaI-NTD. BlaI samples were thus prepared in the same condition at 0.75 mM for ^{15}N -labeled BlaI, 0.5 mM for $^{15}\text{N}/^{13}\text{C}$ -labeled BlaI, and 0.5 mM for $^{15}\text{N}/^{13}\text{C}/^2\text{H}$ -BlaI. For protein interaction studies, two DNA sequences were chemically synthesized: a 30-mer corresponding to the *B. licheniformis* BlaI operator op1 5'-GAA AGT ATT ACA TAT GTA AGA TTT AAA TGC-3', and a consensus palindromic 24-mer DNA: 5'-AAA GTA TTA CAT ATG TAA TAC TTT-3'. DNA was dissolved in the same buffer as the protein. Samples of ^{15}N BlaI and $^{15}\text{N}/^{13}\text{C}$ BlaI-NTD were prepared at a concentration of 0.1 mM. DNA solution was progressively added by amounts of 20 μl to reach BlaI_{dimer}/DNA_{duplex} ratios of 0.5, 1.0, 1.5 and 2.0, and a BlaI-NTD/DNA_{duplex} ratios of 0.5, 1.0, 1.5, 2.0, and 2.5.

NMR spectroscopy

For sequential assignment, standard triple resonance experiments were carried out on ^{15}N and $^{15}\text{N}/^{13}\text{C}$ -labeled samples of BlaI-NTD: HNCA, HNCO, HN(CA)CO, CBCANH, and CBCA(CO)NH for backbone assignment and (H)C(CO)NH-TOCSY, H(CCO)NH-total correlated spectroscopy (TOCSY) for aliphatic side-chain assignment. For resonance assignment of aromatics, HSQC and H(C)CH-TOCSY experiments with the ^{13}C carrier set to 125 ppm, and 2D-NOESY spectrum performed on a sample dissolved in $^2\text{H}_2\text{O}$ were used. An HNCA experiment was performed on a $^{15}\text{N}/^{13}\text{C}/^2\text{H}$ -labeled sample of BlaIGM2 to confirm the assignment of the N-terminal part in the full-length protein.

Inter-protons restraints were derived from NOESY spectra: 2D-NOESY, 3D ^{15}N -edited NOESY-HSQC, regular 3D ^{13}C -edited NOESY-HSQC, 3D ^{13}C -edited NOESY-HSQC optimized for CH groups and 4D ^{13}C -edited HSQC-NOESY-HSQC.²⁶ Mixing times were set to 120 ms.

For chemical shift mapping, ^{15}N -HSQC, ^{13}C -HSQC optimized for aromatics and CT-HSQC were performed at different protein/DNA ratios.

All NMR experiments were performed on Varian INOVA 600 and INOVA 800 spectrometers, both equipped with a triple-resonance (^1H , ^{15}N , ^{13}C) probe and shielded z-gradients. The temperature was set to 25 °C. All triple-resonance experiments used the pulse sequences provided by the Varian Protein Pack.† All data processing, peak picking and peak intensity measurements were performed using the FELIX program version 2000 (Accelrys).

Structure calculation

The NOE distance restraint calibration was performed using cross-relaxation volumes between atoms of known separation in rigid parts of the molecule. A factor of 35% was added to the resulting upper distance, to account for the inherent uncertainty in the distance calculation. Classical pseudo atoms corrections were applied. The lower distance limit was set to the sum of the van der Waals radii of the two protons. Assignment, restraint generation, and structure calculation were performed iteratively. Restraints that were violated, resulting from

† ftp.nmr.varian.com

misassignments or overlapped peaks, were corrected after the first steps of calculation.

The ψ and ϕ angles calculated by TALOS from backbone chemical shift values were used as constraints with lower and upper bounds of $\pm 20^\circ$.²⁷ Structure calculation was carried out using the Discover programs (Accelrys) interfaced to INSIGHTII for visualization and analytical purposes. The force-field used was AMBER.²⁸ The structure determination protocol used a simulated annealing calculation starting from randomized Cartesian coordinates to explore the conformational space, and a restrained molecular dynamics calculation to refine each structure as described.²⁹

Data Bank accession numbers

Chemical shift assignments of *BlaI*-NTD have been deposited with BioMagResBank (accession number 5873). The coordinates of the 19 *BlaI*-NTD refined structures have been deposited in the Protein Data Bank under the accession code 1P6R.

Acknowledgements

This work was supported by the Belgian program of Interuniversity Poles of Attraction initiated by the Federal Office for Scientific Technical and Cultural Affairs (PAI no. P5/33), the "Fonds National de la Recherche Scientifique" (FNRS, Crédit aux chercheurs no 1.5201.02 and FRFC no. 2.4530.03) and the "Communauté Française de Belgique" (projet Tournesol 2003, 03/013). We thank Martin Blackledge for the gift of protocols for structure calculation and for many useful discussions. We also thank Laurence Blanchard for helpful discussion and protein expression protocols. We thank Edwin De Pauw for mass spectrometry analysis.

References

- Charlier, P., Coyette, J., Dehareng, D., Dive, G., Duez, C., Dusart, J. *et al.* (1998). Resistance bactérienne aux β -lactamines. *Medecine/Sciences*, **14**, 544–549.
- Joris, B., Hardt, K. & Ghuysen, J. M. (1994). Analysis of the *penA* gene of *Pseudomonas cepacia* 249. *New Comput. Biochem.* **27**, 505–510.
- Lim, D. & Strynadka, C. J. (2002). Structural basis for the β -lactam resistance of PBP2a from methicillin-resistant *Staphylococcus aureus*. *Nature Struct. Biol.* **9**, 870–876.
- Filée, P., Benlafya, K., Delmarcelle, M., Moutzourelis, G., Frere, J. M., Brans, A. & Joris, B. (2002). The fate of the *BlaI* repressor during the induction of the *Bacillus licheniformis* *BlaP* beta-lactamase. *Mol. Microbiol.* **44**, 685–694.
- Duval, V., Swinnen, M., Lepage, S., Brans, A., Granier, B., Fransen, C. *et al.* (2003). The kinetic properties of the carboxy terminal domain of the *Bacillus licheniformis* 749/I *BlaR* penicillin-receptor shed a new light on the derepression of β -lactamase synthesis. *Mol. Microbiol.* **48**, 1553–1564.
- Filée, P., Vreuls, C., Hermann, R., Thamm, I., Frere, J. M. & Joris, B. (2003). Dimerization and DNA-binding properties of the *Bacillus licheniformis* 749/I *BlaI* repressor. *J. Biol. Chem.* **278**, 16482–16487.
- Wittman, V., Lin, H. C. & Wong, H. C. (1993). Functional domains of the penicillinase repressor of *Bacillus licheniformis*. *J. Bacteriol.* **175**, 7383–7390.
- Joris, B., Hardt, K. & Ghuysen, J. M. (1994). Induction of β -lactamase and low affinity penicillin binding protein 2' synthesis in Gram-positive bacteria. *Bacterial Cell Wall*, **27**, 505–515.
- McKinney, T. K., Sharma, V. K., Craig, W. A. & Archer, G. L. (2001). Transcription of the gene mediating methicillin resistance in *Staphylococcus aureus* (*mecA*) is corepressed but not coinduced by cognate *mecA* and beta-lactamase regulators. *J. Bacteriol.* **183**, 6862–6868.
- Lewis, A. & Dyke, G. H. (2000). *MecI* represses synthesis from β -lactamase operon of *Staphylococcus aureus*. *J. Antimicrob. Chemother.* **45**, 139–144.
- Salerno, A. J. & Lampen, J. O. (1988). Differential transcription of the *bla* regulatory region during induction of beta-lactamase in *Bacillus licheniformis*. *FEBS Letters*, **227**, 61–65.
- Laskowski, R. A., Rullmann, J. A., MacArthur, M. W., Kaptein, R. & Thornton, J. M. (1996). AQUA and PROCHECK-NMR: programs for checking the quality of protein structures solved by NMR. *J. Biomol. NMR*, **8**, 477–486.
- Gajiwala, K. S. & Burley, S. K. (2000). Winged helix proteins. *Curr. Opin. Struct. Biol.* **10**, 110–116.
- Clark, K. L., Halay, E. D., Lai, E. & Burley, S. K. (1993). Co-crystal structure of the HNF-3/fork head DNA-recognition motif resembles histone H5. *Nature*, **364**, 412–420.
- Holm, L. & Sander, C. (1993). Protein structure comparison by alignment of distance matrices. *J. Mol. Biol.* **233**, 123–138.
- Alekshun, M. N., Levy, S. B., Mealy, T. R., Seaton, B. A. & Head, J. F. (2001). The crystal structure of *MarR*, a regulator of multiple antibiotic resistance, at 2.3 Å resolution. *Nature Struct. Biol.* **8**, 710–714.
- Jin, C. & Liao, X. (1999). Backbone dynamics of a winged helix protein and its DNA complex at different temperatures: changes of internal motions in genesis upon binding to DNA. *J. Mol. Biol.* **292**, 641–651.
- Gajiwala, K. S., Chen, H., Cornille, F., Roques, B. P., Reith, W., Mach, B. & Burley, S. K. (2000). Structure of the winged-helix protein hRFX1 reveals a new mode of DNA binding. *Nature*, **403**, 916–921.
- Gregory, P. D., Lewis, R. A., Curnock, S. P. & Dyke, K. G. (1997). Studies of the repressor (*BlaI*) of beta-lactamase synthesis in *Staphylococcus aureus*. *Mol. Microbiol.* **24**, 1025–1037.
- Zheng, N., Fraenkel, E., Pabo, C. O. & Pavletich, N. P. (1999). Structural basis of DNA recognition by the heterodimeric cell cycle transcription factor E2F-DP. *Genes Dev.* **13**, 666–674.
- Lewis, R. A., Curnock, S. P. & Dyke, K. G. (1999). Proteolytic cleavage of the repressor *BlaI* of beta-lactamase synthesis in *Staphylococcus aureus*. *FEMS Microbiol. Letters*, **178**, 271–275.
- Cook, W. J., Kar, S. R., Taylor, K. B. & Hall, L. M. (1998). Crystal structure of the cyanobacterial metallothionein repressor *SmtB*: a model for metalloregulatory proteins. *J. Mol. Biol.* **275**, 337–346.
- Vanzile, M. L., Chen, X. & Giedroc, D. P. (2002). Structural characterization of distinct alpha3N and

- alpha5 metal sites in the cyanobacterial zinc sensor *Smtb*. *Biochemistry*, **41**, 9765–9775.
24. Filée, P., Delmarcelle, M., Thamm, I. & Joris, B. (2001). Use of an ALFexpress DNA sequencer to analyse protein–nucleic acid interactions by band shift assay. *Biotechniques*, **30**, 1044–1051.
25. Lepre, C. A. & Moore, J. M. (1998). Microdrop screening: a rapid method to optimize solvent conditions for NMR spectroscopy of proteins. *J. Biomol. NMR*, **12**, 493–499.
26. Kay, L. E., Clore, G. M., Bax, A. & Gronenborn, A. M. (1990). Four-dimensional heteronuclear triple-resonance NMR spectroscopy of interleukin-1 β in solution. *Science*, **249**, 411–414.
27. Cornilescu, G., Delaglio, F. & Bax, A. (1999). Protein backbone angle restraints from searching a database for chemical shift and sequence homology. *J. Biomol. NMR*, **13**, 289–302.
28. Pearlman, D. A., Case, D. A., Caldwell, J. C., Seibel, G. L., Singh, U. C., Weiner, P. & Kollman, P. A. (1995). *Amber 4.1*, Department of Pharmaceutical Chemistry, University of California, San Francisco, CA.
29. Cordier, F., Caffrey, M., Brutscher, B., Cusanovich, M. A., Marion, D. & Blackledge, M. (1998). Solution structure, rotational diffusion anisotropy and local backbone dynamics of *Rhodobacter capsulatus* cytochrome c2. *J. Mol. Biol.* **281**, 341–361.

Edited by P. Wright

(Received 21 July 2003; received in revised form 1 September 2003; accepted 5 September 2003)

SCIENCE  DIRECT®
www.sciencedirect.com

Supplementary material comprising two figures is available on Science Direct